Source of the Ice-Binding Specificity of Antifreeze Protein Type I

Pranav Dalal and Frank D. Sönnichsen*

Department of Physiology and Biophysics, Case Western Reserve University, 10900 Euclid Avenue, Cleveland, Ohio 44106-4970

Received March 20, 2000

Antifreeze proteins (AFPs) are a group of structurally very diverse proteins with the unique capability of binding to the surface of seed ice crystals and inhibiting ice crystal growth. The AFPs bind with high affinity to specific planes of the ice crystal. Previously, this affinity of AFPs has been ascribed to the formation of multiple hydrogen bonds across the protein−ice interface, but more recently van der Waals interactions have been suggested to be the dominant energetic factors for the adsorption. To determine whether van der Waals interactions are also responsible for the binding specificities of AFPs, the protein−ice interaction of the helical AFP Type I from winter flounder (HPLC6) was studied using a Monte Carlo rigid body docking approach. HPLC6 binds in the $\{1\bar{1}0\bar{2}\}$ direction of the $[20\bar{2}1]$ plane, with the Thr-Ala-Asn surface comprising the protein's binding face. The binding of HPLC6 to this ice plane is highly preferred, but the protein is also found to bind favorably to the $[10\bar{1}0]$ prism plane using a different protein surface comprised of Thr and Ala residues. The results show that van der Waals interactions, despite accounting for most of the intermolecular energy (>80%), are not sufficient to completely explain the AFP binding specificity.

INTRODUCTION

Fish antifreeze proteins (AFPs) are a class of structurally diverse proteins that protect polar fish from fatally freezing in ice-laden environments, where the temperature of seawater is about 1 °C below the freezing point of the fish's body fluids. The proteins are present in fish serum and certain tissues such as gills, fins, and skin. AFPs depress the freezing point of their solutions in a kinetic, noncolligative manner, brought about by AFP adsorption to specific surface planes of seed ice crystals. This adsorption inhibits further growth of the ice-seed[1] and effectively lowers the freezing point of the fish's body fluids from −0.8 °C to about −2 °C. Five different types of fish AFPs are known to date.[2] They are very divergent in size and structure but seem to function similarly. Of these proteins, AFP type I is the most studied antifreeze protein, particularly the liver-isoform from winter flounder (HPLC6). This monomeric, alanine-rich protein is comprised of 37 amino acids, containing three 11-amino acid repeats (TA_2NA_7) and additional N- and C-terminal capping sequences. It folds into a single, fairly straight α-helix,[3] in which all polar residues with the exception of one Glu-Lys salt bridge are located on one side of the helix. Several studies using residue replacements indicated the protein's ice binding site and supported the involvement of hydrophilic residues in ice-binding.[4] These Thr and Asn residues are regularly spaced with 16.5 Å separation.[5] The distance almost ideally matches the ice structure periodicity of 16.7 Å in the protein's adsorption direction in the adsorption plane (the $\{1\bar{1}0\bar{2}\}$ direction in the $[20\bar{2}1]$ plane). [Numbers in square brackets represent the family of 12 symmetry related planes in the hexagonal, four axis system identified by the Miller indices of one selected plane. Directions of binding are given as vectors in curly brackets, again referring to all symmetry related directions. For consistency, the selected vector represents the absolute direction in the respective, selected plane and is defined as the vector along the helical axis of the HPLC6 from the N- to the C-terminus.] Both the direction and plane have been determined experimentally by ice-etching studies.[6] The distance match supported the hypothesis that AFP−ice binding is mediated primarily by the formation of multiple hydrogen bonds between the protein and ice surface.[7]

More recently, the presumed critical role of hydrogen bonds in the adsorption of AFPs to ice has been questioned. A detailed analysis of the solution structure of AFP type III and its ice-bound model[8] suggested a significant role of hydrophobic interactions in the AFP−ice adsorption. Conclusive experimental evidence for the importance of van der Waals interactions was obtained by systematic Thr replacements in HPLC6.[9] Isosteric Val analogues were found to be highly active, whereas Ser analogues were practically inactive despite the retained hydrogen bonding capacity in their side chain. These results and subsequent studies[10,11] strongly suggested that van der Waals interactions are primary determinants of HPLC6−ice interaction, while hydrogen bonds energetically play a minimal role in the protein−ice adsorption. Furthermore, very recent systematic Ala to Leu replacements around the helix have proposed an alternate protein binding face comprised of the Thr residues and two equivalent Ala positions (Thr-Ala-Ala) along the helix.[12] This surface is rotated by 90° relative to the putative Thr-Ala-Asn adsorption face. These recent results demonstrate the limits of our current understanding of the HPLC6−ice binding mechanism and suggest the need for a reconsideration of mechanistic aspects, such as the role of hydrophobic versus hydrophilic interactions, the location of the protein's ice binding surface, and the source of its orientational and planar specificity.

* Corresponding author. Phone: (216) 368-5405. Fax: (216) 368-1693. Email: frank@herring.phol.cwru.edu.

10.1021/ci000449b CCC: $19.00
Published on Web 08/06/2000

Due to the experimental difficulties in studying ice-bound AFP structures, various groups[13−16] have modeled the AFP−ice interactions using computational approaches. Common features of these modeling studies are (a) manual placement of the protein in selected orientations, (b) a primary focus on hydrogen bonds, and (c) modeling to only the [20$\bar{2}$1] ice plane with a predefined binding face. Wen and Laursen[13] and Madura et al.[15] proposed that HPLC6 favorably binds to ice in the {1$\bar{1}$0$\bar{2}$} direction on the [20$\bar{2}$1] ice plane with the N-terminus pointing toward the *c*-axis apex ({1$\bar{1}$0$\bar{2}$} or N+), compared to the mirror symmetry direction ({01$\bar{1}\bar{2}$}) and their respective 180° rotations ({$\bar{1}$102} and {0$\bar{1}$12}). In their model, Thr and Asn residues bind to different ranks of oxygen on the ridge of the [20$\bar{2}$1] plane, as opposed to a model proposed by Sicheri and Yang[5] in which Thr and Asn bind to the same rank of oxygen. Recently, Cheng and Merz[16] completed a study using molecular dynamics calculations including the effects of water. The authors confirmed Wen and Laursen's model[13] and further suggested a correlation between experimentally observed antifreeze activities and binding energies or the number of protein−ice hydrogen bonds.

A model developed using a Monte Carlo approach to automatically identify the preferred binding position of HPLC6[14] agreed with the model by Wen and Laursen.[13] Further, AFP binding to the [20$\bar{2}$1] plane was favored relative to the basal plane ([0001]) binding. The source of this plane specificity originated in larger favorable van der Waals interactions in the [20$\bar{2}$1] plane, whereas contributions from hydrogen bonds and charge interactions to the intermolecular energies were similar.

The suggested importance of hydrophobic interactions also leads to the need to reevaluate the current protein−ice models. In the absence of hydrogen bonds, these models do not necessarily explain the protein's ice affinity and specificity of binding. Further, the current studies have only investigated the Thr-Ala-Asn protein surface, and the properties of the alternative binding site adsorbing to ice have yet to be modeled. Thus, the focus of this study is to generate unbiased ice-bound protein models using a Monte Carlo rigid body docking procedure. The protein is modeled to several ice surface planes in order to identify the source of the protein's directional and orientational specificity and to determine the preferred ice-adsorption surface of the protein.

METHODS

Initial coordinates for HPLC6 were taken from the crystal structure.[5] An analysis of these coordinates (PDB accession codes 1WFA and 1WFB) showed variable degrees of helix bending of the two AFP molecules in the unit cells. Therefore, idealized straight helices with ϕ and ψ angles of −65° and −41.6°, respectively, were generated, which reproduced the approximate 11-amino acid repeat observed in the crystal structures. Side chain conformations were obtained from the deposited coordinates. Alternative Thr side chain rotamers were generated manually in Insight II (MSI, San Diego, CA) from this template. The resulting protein structure was minimized for 1000 steps with fixed backbone. The details of the minimization are described below.

An I_h unit cell was constructed with TIP3P water molecules. Ice lattices (approximate dimensions of 80 Å × 65 Å × 10 Å) were then obtained by repetition of this I_h unit cell by a Fortran program and were subsequently cut to obtain the desired crystallographic surface. The choice of the exact location of the cut results in planes with identical indices but differing surface properties. Four different [20$\bar{2}$1] planes can be generated, each with a different surface. After estimating the plane stability using the number of broken hydrogen bonds, and the number of hydrogen bonds per surface water molecule, two planes were selected. The plane with the smallest number of broken hydrogen bonds (5) was selected for this study ([20$\bar{2}$1], different cut), although it has not been used for modeling studies so far. The only other plane ([20$\bar{2}$1]), in which all surface water molecules are involved in at least two hydrogen bonds, is identical to the [20$\bar{2}$1] plane used in previous modeling studies by Wen and Laursen.[13] Another plane, parallel but slightly different from the ones utilized here, has been previously used in another study.[15] This plane might be considered to be the ideal [20$\bar{2}$1] plane, since it intersects a unit cell exactly at the positions defined by the Miller indices or reciprocal coordinates. This plane, however, seems less realistic as one water molecule is bonded to the lattice only via a single hydrogen bond. Similar selections were made for the prism and the basal plane, while only one possible cut exists for the secondary prism plane.

The docking algorithm used for these calculations is implemented in the Insight II (MSI) software. For energy evaluations in the docking calculations and the minimizations, the all-atom constant valence force field (CVFF) was used. A simplified energy expression was employed consisting of bonded interactions, and van der Waals interactions as the only nonbonded interactions. The van der Waals energies were calculated using the cell multipole method,[17] with the Insight II implementation specific parameters set to single energy evaluation and coarse accuracy. Oxygen atom positions of the ice were kept fixed throughout the calculations using a subset definition. The intermolecular energy was calculated as the difference between the total energy of the system (protein and ice) and the sum of individual energies of ice and protein.

The MC_Minimize docking algorithm used in these calculations is implemented in the fixedDocking command, part of the Affinity module in the Insight II software. The algorithm uses alternating random rigid body moves of a ligand and energy minimization of the system to identify the favorable conformations. The energy minimization step in this algorithm utilizes the Discover 95.0/3.00 program implemented in the Discover_3 module of Insight II. The docking algorithm was slightly modified, a R. M. S. check that was originally placed after the minimization was moved to before the minimization in order to avoid unnecessary minimizations, and thus saving on the computational cost. Details of the algorithm are given in Figure 1.

For each step of the calculations, the protein alignment relative to the ice was altered by a Monte Carlo rigid body move of the protein. This move, which had 6 degrees of freedom, consisted of random translations of the protein in all three directions of the ice-crystal coordinate system and random rotations around the three principal axes of the protein. Subsequently, an energy and a root mean square check were performed. To avoid minima trapping, instead of a Metropolis energy acceptance criterion, a more generous

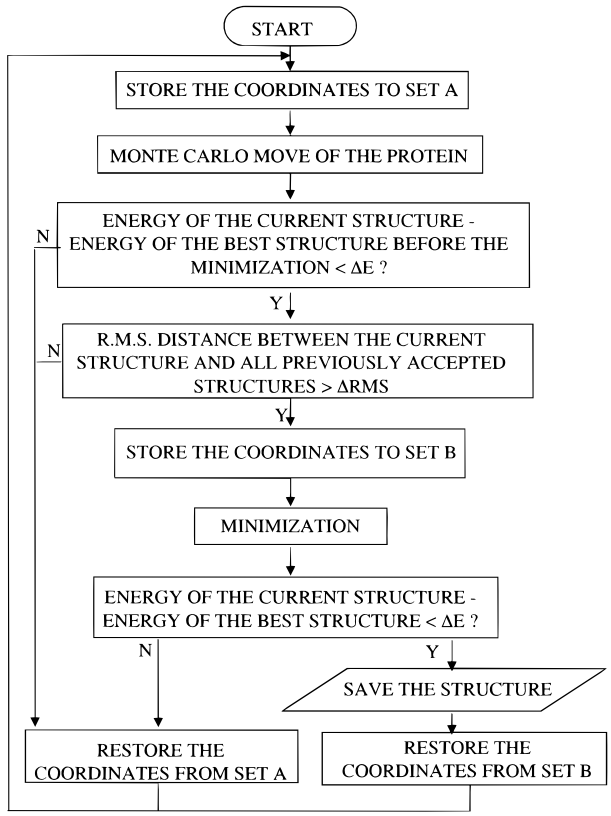

Figure 1. Flow chart of the algorithm employed in the calculations. The MC_Minimize algorithm implemented in the Affinity module of the Insight II software was used for the calculations. It was slightly modified for these particular calculations. The modified algorithm is described in the text.

energy range criterion was used. New structures with energies up to a specified number (ΔE) of kilocalories per mole less favorable than the best accepted structure were accepted. The root mean square check ensured that the root mean square (RMS) distance between the current and all previously accepted protein structures was greater than a specified number (ΔRMS) of angstroms. After passing these two checks, a conjugate gradient energy minimization was performed. If the minimized structure passed the energy check, it was saved for analysis. Independent of this acceptance, the protein geometry was restored to the (idealized) starting protein geometry after each minimization before the next Monte Carlo move.

A typical calculation used two phases: the purpose of the first phase was the identification of a global minimum by an extensive search of the alignment space. Rotational and translational moves were allowed on all three axes, and randomly selected from -180 to $+180°$ and -6 to $+6$ Å. A root mean square criterion (ΔRMS $>$ 1.5 Å) and an energy criterion (ΔE $<$ 5 kcal/mol) were used to prescreen the new alignment, ensuring that only significantly different structures with better or similar energies were subjected to a 100 steps conjugate gradients minimization. After minimization, the energy criterion (ΔE $<$ 5 kcal/mol) was again employed for final acceptance of the alignment. The end of phase I, usually reached after about 250 000 iterations, was indicated by the repetitive nature of the solutions. At this point, accepted structures represented equivalent models, but with translated protein adsorption positions on the ice. To further optimize the protein alignment on the ice, the root mean square criterion was removed, and its rotational and translational movements were restricted ($<5°$ and <0.5 Å). Along with narrower energy criteria before (ΔE $<$ 2 kcal/mol) and after (ΔE $<$ 0 kcal) minimization (200 steps of conjugate gradients) these changes resulted in a rapid descent to the energetic minimum of the identified alignment. Once the energy value of the accepted structures remained constant, and no further structures were accepted for 10 000 calculations steps, the lowest energy structure was selected for a 1000 step conjugate gradients minimization.

To test for the influence of the computational parameters on the calculation results, the final accepted structures were minimized in the presence of charge interactions with different force fields (AMBER and cff91), with a range of 1−20 Å van der Waals interaction cutoffs (instead of the cell multipole method), and with different treatments of the dielectric constant (1, 1*r, 4, 4*r). The obtained intermolecular energies may differ by 100% depending on the respective parameters. However, ranking of the different models based on their intermolecular energies was identical irrespective of the choice of the parameters.

Excluded accessible surface areas (EASAs) for the models were calculated in the program GRASP,[18] using heavy atoms and a default probe radius of 1.4 Å. For the protein, contributions of oxygen and nitrogen atoms were summed to yield the polar EASA, while the carbon EASA yielded the nonpolar contribution.

RESULTS

The docking of HPLC6 to several ice−surface planes using the Monte Carlo method yielded strongly preferred protein alignments in all cases. In the following, the time course and properties of the calculation for HPLC6 and the $[20\bar{2}1]$ plane are discussed in detail, as these results are representative for all employed calculations. A set of 254 690 Monte Carlo protein alignments was evaluated, of which most were rejected by the energy and root mean square criteria. Figure 2A shows the energy of the 303 structures accepted throughout the simulation, and parts B and C of Figure 2 depict the geometric properties of those accepted structures. These properties together with selected structures from the simulation (Figure 2D) illustrate the achieved broad conformational search.

From the starting point, in which the protein is placed farther than 10 Å from the ice surface, the total energy decreases gradually (Figure 2A). Since the intramolecular energies for ice and protein remain nearly constant (data not shown), this energy decrease reflects the increase in favorable intermolecular van der Waals interactions. Distinctive drops in the energy can be observed. The first drop (structure 99) indicates the end of the approach of the protein toward the ice surface. In all subsequent structures the protein is aligned with the long helical axis parallel to the ice surface. This is evident from an analysis of Thr distances to the ice surface (Figure 2B) and the angle between the ice surface plane and the protein's putative ice binding surface (Figure 2C). Both these properties are initially strongly varying. From structure 99 onward, Thr−ice distances behave cooperatively and are small (3 and 10 Å). Three distinct protein surface−ice surface angles are observed (10, 50, and 90°), representing three different protein surfaces being in contact with ice. One of

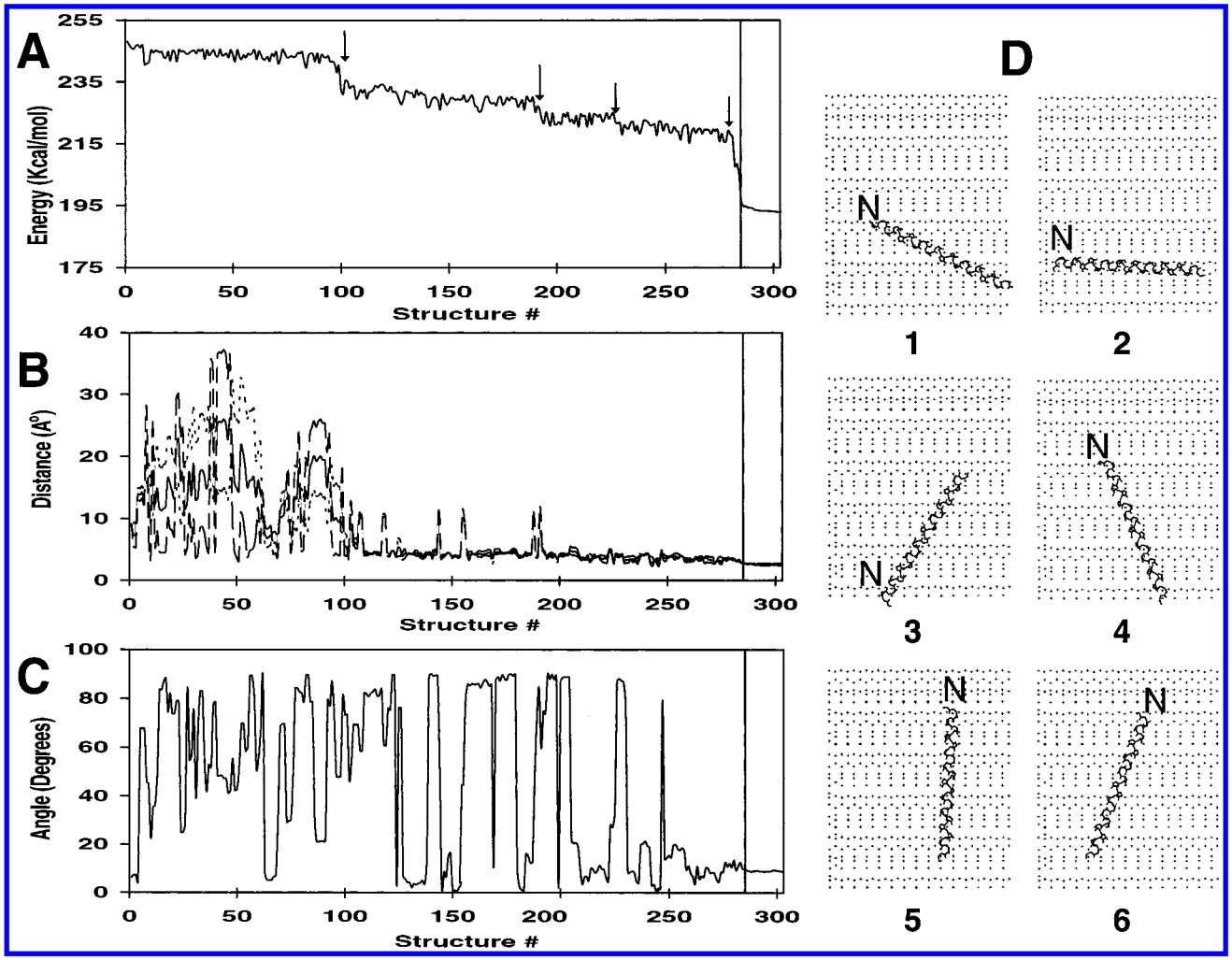

Figure 2. Properties of the docking simulation of HPLC6 ($\chi_1 = -60°$) onto the [20$\bar{2}$1] ice plane. The *x*-axis represents the structure number in A, B, and C. The line in the graphs indicates the start of phase II of the conformational search. (A) Total energy of the system (ice and protein) during the conformational search. (B) Distances of three Thr residues (Thr 13-dotted line, Thr 24-solid line, and Thr 35-dashed line) to the ice plane. (C) Angle generated between the protein (plane of the protein defined by Thr 13, Thr 24, and Asn 16) and the ice surface plane. (D) Selected structures obtained during the conformational search (structures 190, 209, 213, 217, 252, 294). Structure 3 is the binding of HPLC6 with the N-terminus facing away from the *c*-axis {$\bar{1}$102}, whereas structure 4 is the mirror binding direction of {1$\bar{1}$02} i.e., {01$\bar{1}$2}. Structure 6 is the final conformation of the phase I in which the HPLC6 binds in the {1$\bar{1}$02} direction of the [20$\bar{2}$1] ice plane.

these protein surfaces is comprised of Leu and adjacent Ala residues and is characterized by the 10 Å Thr distance to the ice, and a protein surface−ice surface angle of 50 ± 30°. Models using this adsorption surface are accepted until structure 192; upon its exclusion a small decrease in energy is observed. The other observed surface plane angles of 10 and 90° exhibit very similar Thr−ice distances (Figure 2B). These values characterize two putative protein adsorption surfaces: the previously accepted surface comprised of Thr, Ala, and Asn residues, and the proposed alternative binding face that is comprised of the conserved Ala-face and the adjacent Thr residues.[12] The latter occurred with significant frequency up to structure 230. However, coinciding with a small drop in the total energy, all following structures (with one exception) adsorb to ice with the Thr, Ala, and Asn surface.

Concurrent with the selection of a preferred protein adsorption face, specific protein orientations are selected. Nevertheless, following structure 230 three different orientations were accepted. These include the expected binding direction, i.e., the protein binding in the {1$\bar{1}$0$\bar{2}$} direction with the N-terminus pointing toward the apex, the opposite direction with the N-terminus facing away from the apex ({$\bar{1}$10$\bar{2}$} or N-), and the mirror protein binding direction ({01$\bar{1}$$\bar{2}$}). However, the latter two orientations are last accepted at structures 274 and 258, respectively.

The largest drop in energy of about 10 kcal/mol was observed near the end of phase I (structure 282). This energy decrease is due to the structure finding its optimum alignment. In all subsequent structures, the protein is translationally displaced but found in equivalent adsorption positions, a consequence of the repetitive nature of the ice surface. The fact that the protein translates by multiples of crystallographic units without finding different solutions with similar energies indicates that this conformational search identified the globally best adsorption alignment. Therefore, the procedure was modified at this point (see Methods). With only small rotational and translational adjustments allowed, the protein further optimized into the alignment (structures 285−303), which yielded another 10 kcal/mol reduction in total energy.

The final model of HPLC6 adsorbing to the [20$\bar{2}$1] plane is visualized in Figure 3. The protein aligns along the {1$\bar{1}$0$\bar{2}$}

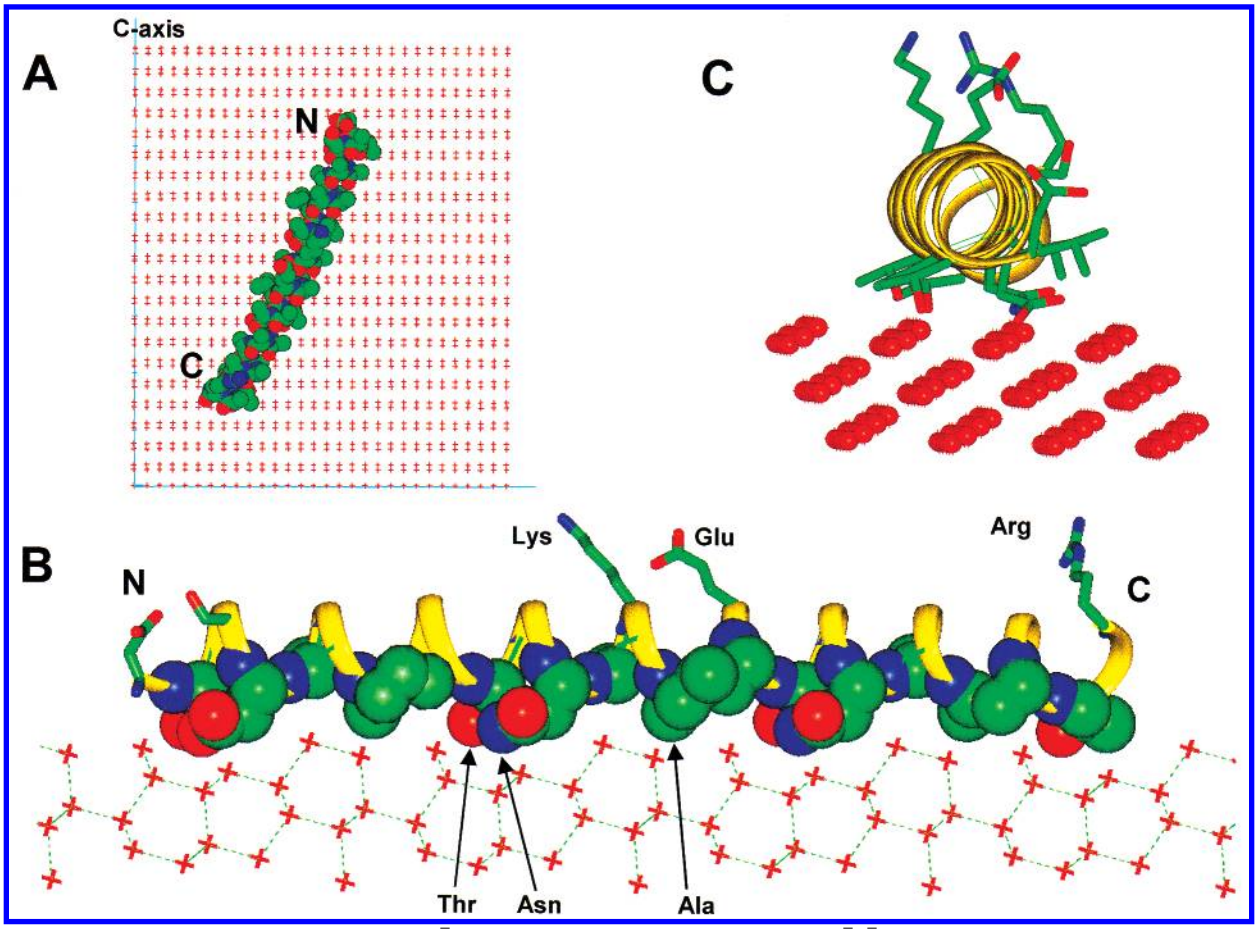

Figure 3. Model of HPLC6 adsorbing to the [20$\bar{2}$1] ice plane. The protein binds in the {1$\bar{1}$0$\bar{2}$} direction. (A) Top view normal to the ice plane. The N-terminus is located at the top (toward the *c*-axis). (B) Space filling model, showing the structural fit between the ice plane and the protein. Shorter side chains of Ala sit on the ridge and Thr and Asn side chains fit into the valley, whereas the bulkier side chains (Lys, Glu and Arg) face away from the ice. (C) Helical view looking directly at the C-terminus of the protein. Overall helicity of the protein is maintained in this final conformation. The red spheres indicate the oxygen atoms of the water in the ice crystal.

direction, so that the N-terminus is located toward the bipyramidal apex (N+ conformation). A match is observed between the 16.5 Å distance of equivalent 11-residue spaced residues and the ice structure periodicity of 16.7 Å in this direction. This places equivalent residues in the protein's adsorption site in equivalent positions on the ice surface. The space-filling model highlights the ridge and valley topology of this ice surface plane. Bulkier, nonrepeated side chains (Lys18, Glu22, and Arg37) face away from the protein's binding face. Thr and Asn not only face the ice, their side chains fit into the valleys or grooves of this particular ice surface, while shorter Ala side chains sit on the ridges (Figure 3B). Little changes in overall helicity are observed (Figure 3C). The displayed surface complementarity leads to a close proximity between protein and ice surface and a relatively large density of atoms at the interface. The surface complementarity between protein and ice is also presented in Figure 4 by directly visualizing the molecular surfaces of the protein and ice. The surface to surface distance in the protein−ice interface is generally less than 2.5 Å, and a large proportion of the protein surface is in direct van der Waals contact with the ice. The match of the corrugated surfaces can be quantified in terms of EASA between the protein and ice (Tables 1 and 2).

The only residues in contact with ice that have variable side chain conformations are the putative ice-binding residues Asn and Thr. In the final model, their side chain angles are close to the original values, chosen at the start of the calculations on the basis of the crystal structure. Therefore we investigated whether these are the preferred rotamers in the ice bound model or whether alternative conformations would be compatible. The χ_1 angle of the Asx rotamers was changed from −60° to +60° and +180° during the last minimization (see Methods) with charge interactions included. Although the data for different χ_2 values are not shown, there was no effect of changing χ_2 angles on intermolecular energies or EASA. No significant change in intermolecular energy or EASA is observed among the three rotamers (Table 1). The χ_1 angles of all Thr residues in the protein were similarly changed to +60° and −180°, and independent docking calculations were performed. The resulting models are nearly identical to wild type ($\chi_1 = -60°$) with root mean square displacements of <1 Å for both pairwise comparisons. The intermolecular energy of binding is less favorable for the +60° rotamer (−54.4 kcal/mol) compared to the −60° (−67.2 kcal/mol) and 180° (−64.8 kcal/mol) rotamers (Table 1). With the van der Waals component of the intermolecular energy being similar in all three models, the intermolecular Coulomb energy is less favorable in the +60° rotamer. This reflects the absence of hydrogen bonds for the Thr residues in this model, a consequence of the inappropriate positioning of Thr side

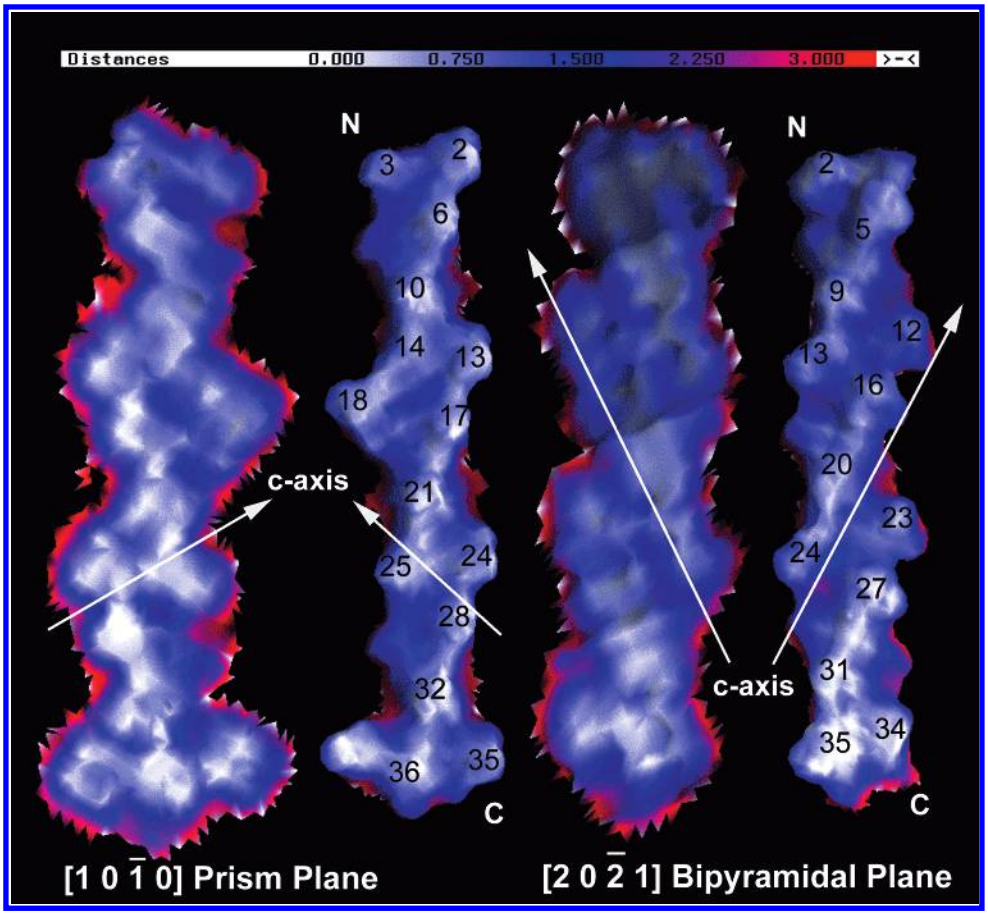

Figure 4. Excluded molecular surfaces of the HPLC6−ice complex models. The molecular surfaces of ice and the protein are shown on the left and right for HPLC6 bound to the [20$\bar{2}$1] and [10$\bar{1}$0] ice planes, respectively. The surfaces were calculated for the respective complex structure in GRASP.[18] The protein was subsequently rotated by 180° and displaced to allow a concurrent view at both the protein and ice excluded surfaces. Residue numbers highlight the protein residues in contact with ice, and the relevant residue spacings that match surface indentations along crystallographic axes in the respective ice planes (i,i+3 in the [10$\bar{1}$0] plane) and i,i+4 in the [20$\bar{2}$1] plane). Arrows indicate the orientation of the c-axis of hexagonal ice I_h. The applied color gradient from white via blue to red represents distances between protein and ice surfaces in the complex from 0 Å (direct contact) over 1.4 Å (water inaccessible) to 3 Å.

Table 1. Effect of Thr and Asn Rotamers on Binding of HPLC6 to the [20$\bar{2}$1] Ice Plane

	intermolecular energy (kcal/mol)				excluded accessible surface area (Å^2)			
	without charges	with charges			protein			
rotamers	vdW/total	vdW	Coulomb	total	nonpolar	polar	ice	total
Thr (−60°) and Asn (−60°)	−60.7	−55.9	−11.3	−67.2	554	441	832	1827
Thr (+60°)	−57.7	−53.9	−0.5	−54.4	636	295	770	1701
Thr (180°)	−59.9	−56.0	−8.8	−64.8	512	455	819	1786
Asn (+60°)	−57.8	−54.5	−10.2	−64.7	529	432	801	1762
Asn (180°)	−60.6	−51.8	−13.1	−64.9	516	485	800	1801

Table 2. HPLC6 Binding to Different Ice Planes

	intermolecular energy (kcal/mol)				excluded accessible surface area (Å^2)			
	without charges	with charges			protein			
plane	vdW/total	vdW	Coulomb	total	nonpolar	polar	ice	total
[20$\bar{2}$1]	−60.7	−55.9	−11.3	−67.2	554	441	832	1827
[20$\bar{2}$1] Thr-Ala-Ala	−49.1	−47.1	−2.9	−50.1	685	194	734	1613
[20$\bar{2}$1] (a different cut)	−51.4	−48.1	−6.3	−54.4	547	314	686	1547
[10$\bar{1}$0] prism	−64.3	−64.4	−1.6	−66.0	705	258	801	1764
[0001] basal	−47.5	−51.2	1.6	−49.6	656	194	714	1564
[11$\bar{2}$0] secondary prism	−49.2	−50.6	0.5	−50.1	665	201	745	1611

chain atoms relative to the ice coordinates. On the other hand, the 180° rotamer model is nearly indistinguishable from the −60° model in all properties such as van der Waals and Coulomb contributions to the inter- and intramolecular energies. Moreover, the Thr residues exhibit hydrogen bonds in both of these models, albeit to different water molecules in the ice plane. Overall, surprisingly little preference for specific rotamer populations is observed in this study. The

ice environment accommodates quite different side chain conformations and does not impose a steric restriction on the Thr and Asn side chains.

The [20$\bar{2}$1] plane is the experimentally observed adsorption plane for HPLC6.[6] A steric complementarity, highlighted by a 16.7 Å periodicity found in both the protein and the ice, has been made responsible for the experimentally observed specificity. However, other planes with a similar 16.7 Å periodicity are present in the ice crystal that could serve as adsorption planes. One of these, the secondary prism plane, was found to be the adsorption plane for a HPLC6 analogue, in which all four Thr residues were replaced by Ala[10] and for a helical AFP isoform from sculpin.[19] Since these proteins still have the same periodicity, the actual source for binding specificity is unclear. To gain more insight, docking studies as presented for the [20$\bar{2}$1] plane were repeated for a selection of other crystallographic planes. Favorable models were selected and minimized using different parameters and force fields. Presented are results for two sets of calculations: minimization in the absence and presence of charge interactions (Table 2). These results are nearly identical since the Coulomb energies, when calculated, are significantly smaller than the van der Waals energies in all models.

Intermolecular energies for a different cut of the [20$\bar{2}$1] plane, the secondary prism plane ([11$\bar{2}$0]) and the basal plane ([0001]) are significantly higher (>10 kcal/mol) than the [20$\bar{2}$1] plane (Table 2). Similarly, the EASAs for these models are substantially smaller than 1827 Å^2 for the [20$\bar{2}$1] plane. This indicates significantly less surface complementarity between protein and ice in these models and suggests that these three planes are inferior adsorption planes.

Surprisingly, the protein exhibits favorable binding to the prism plane ([10$\bar{1}$0]). The prism plane model is comparable in most aspects to the [20$\bar{2}$1] model. Its excluded accessible surface area is 1764 Å^2, and its van der Waals energy is similar, or up to ~8 kcal/mol more favorable, depending on the force fields and calculation parameters. On the other hand, the electrostatic component in the prism plane model is very small. This largely compensates for the increased van der Waals interactions, so that the total energy of the prism plane model is very similar to that of the [20$\bar{2}$1] plane model. Further, the surface complementarity of both models is qualitatively comparable (Figure 4). Common features are the surface ridges created by four-residue spaced side chains and the ridge separation by about 17 and 4 Å in the direction and orthogonal to the helical axis, respectively. Only subtle differences are observed for the actual length of these ridges, and the angle between them. The similarity is very surprising in light of the models utilizing different adsorption faces. As shown, the model of HPLC6 binding to the [20$\bar{2}$1] plane utilizes the Thr-Ala-Asn face. On the other hand, the prism plane model utilizes the recently proposed alternate Thr-Ala-Ala binding face.[12] This respective, very nonpolar protein surface is rotated by 90° relative to the Thr-Ala-Asn binding face. It is noteworthy that almost all models utilize this binding face. Also, during the [20$\bar{2}$1] plane calculations, this adsorption face is sampled and accepted, but it is eventually excluded in favor of the putative Thr-Ala-Asn face. To facilitate a comparison between the properties of both protein surfaces in binding to the [20$\bar{2}$1] planes, the energetically most favorable structure utilizing the Thr-Ala-Ala face and binding in the {1$\bar{1}$0$\bar{2}$} direction was taken from the [20$\bar{2}$1] plane calculations. This structure was then subjected to phase 2 of the procedure for optimization (see Methods). Nevertheless, the resulting model of the protein adsorbing with the Thr-Ala-Ala face to the [20$\bar{2}$1] plane is less favorable. Expectedly, the intermolecular Coulomb interaction is very small due to the nonpolarity of the protein surface (73% nonpolar) and the consequential absence of hydrogen bonds in this adsorption model. In total, the intermolecular energy for this model is 17 kcal/mol, and the EASA is 214 Å^2 smaller than the respective values for the putative Thr-Ala-Asn face (Table 2). The Thr-Ala-Ala binding face seems to be a significantly less suitable surface of HPLC6 to adsorb to the bipyramidal [20$\bar{2}$1] ice plane.

DISCUSSION

The generally employed manual initial placement of HPLC6 on the ice surface has the potential to lead to input-biased results. Such placement not only fixes the expected protein-adsorption face but may also impact on the protein's final adsorption position on the ice lattice due to inefficient protein translation or rotation during the calculation. An essential focus of this study was therefore to overcome these limitations and reduce the inherent assumptions and the possibility of biased results as far as possible. One previous study[14] modeled the HPLC6−ice interaction by Monte Carlo rigid body docking. This methodology, involving random translational moves and rotations of a ligand, is ideally suited to eliminate initial AFP placement bias and to reliably and completely search the relative alignment space between protein and ice. To further reduce the possibility of procedure artifacts, the Monte Carlo search used van der Waals interactions as the primary acceptance criterion, while final models were minimized using a variety of force fields and parameters.

As described in detail, the designed modeling procedure is capable of searching the relative protein alignments on the ice and yields low-energy protein−ice complex models that are independent of the initial protein placement. The calculations converge to a group of nearly identical structures, despite the relative flatness of the ice surface and the consequential shallowness of the energy surface. The variability in the initial structures versus the similarity of the best solutions differing only by translation along the crystal unit directions (reflective of the presence of multiple identical binding sites due to the repetitiveness of the crystal surface) demonstrates the success of the method in searching protein alignments on the ice. As expected, protein surfaces of primarily planar character and of significant surface area are found in contact with ice as they lead to larger favorable intermolecular van der Waals attraction. The most favorable models exhibit close proximity between HPLC6 and ice, facilitated by a complementarity in the respective surface corrugations.

The described modeling method identified the {1$\bar{1}$0$\bar{2}$} direction as being strongly preferred for the binding of HPLC6 to the [20$\bar{2}$1] plane of ice. This direction correlates well with the experimental data obtained by ice-etching studies[6] and previous modeling studies.[13−16] Similar to the observed directional specificity within a given plane, van der Waals interactions lead to significant differences in intermolecular energies between the HPLC6 and various ice

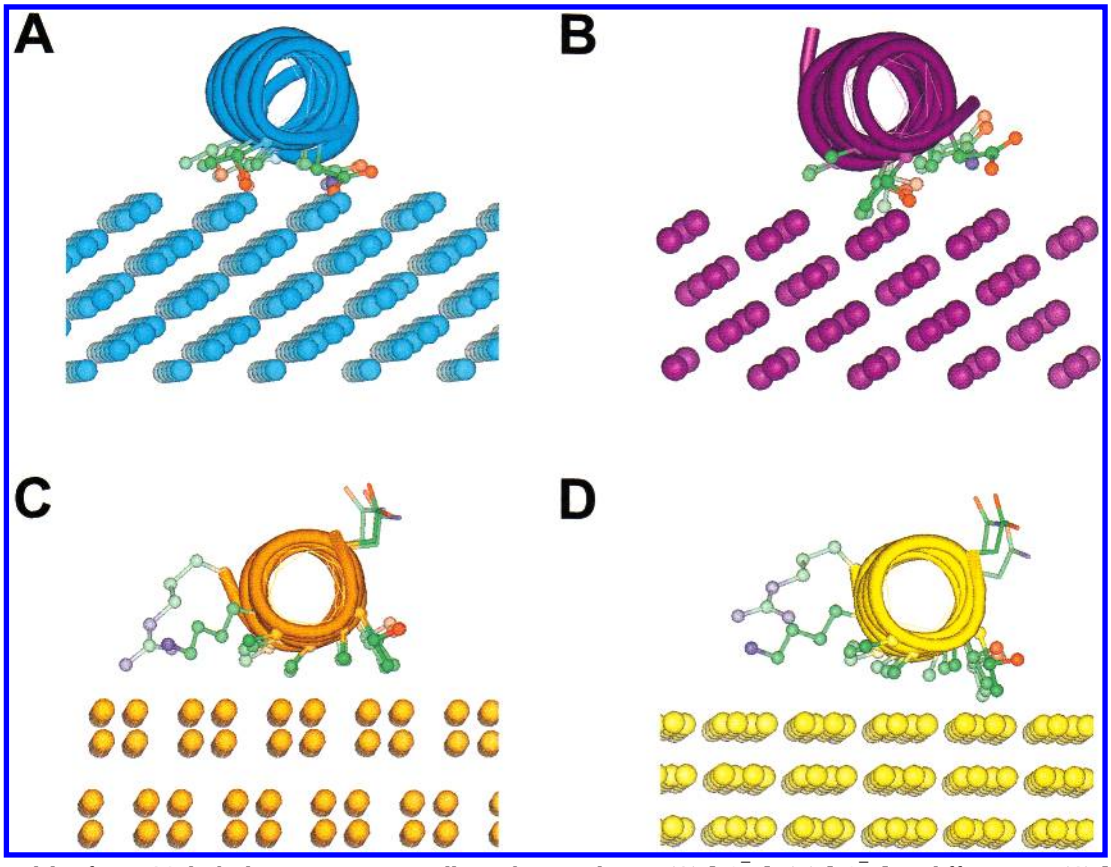

Figure 5. Models of HPLC6 docked onto various crystallographic ice planes: (A) [20$\bar{2}$1]; (B) [20$\bar{2}$1]—a different cut; (C) [10$\bar{1}$0] prism plane; (D) [11$\bar{2}$0] secondary prism plane. Oxygen atoms of ice in these planes are shown in CPK presentation. Protein backbone atoms, side chains interacting with ice, and Asx side chains are shown in ball-and-stick presentation.

planes (Figure 5). Basal, secondary prism, and a differently cut [20$\bar{2}$1] plane lack the surface complementarity observed for HPLC6 and the [20$\bar{2}$1] plane, resulting in significantly less favorable intermolecular energies. This again supports the notion that van der Waals interactions are largely responsible for the positional specificity of HPLC6. On the basis of van der Waals energetic criteria alone, however, prism plane binding of the protein was comparable to the binding to the [20$\bar{2}$1] plane. The latter is more stable; i.e., agreement between calculations and experiments is found only if charge interactions are included. Although the resulting energies are relatively small in magnitude, these contributions may be the discriminating factor between these two models, which could lead to the bipyramidal plane adsorption being most favorable overall. Thus, in these calculations van der Waals interactions are not sufficient to reproduce the known adsorption specificity of this AFP.

One observation is noteworthy. While, [20$\bar{2}$1] utilizes the protein face comprising Thr-Ala-Asn, the Thr-Ala-Ala face is the protein's ice adsorption face in the prism model. This latter face is rotated 90° relative to the Thr-Ala-Asn face and has recently been proposed to be the protein's adsorption face.[10] This hypothesis received strong experimental support recently. The Baardsnes et al. face[12] could show that Ala to Leu replacements in this face renders the protein inactive, while similar replacements in other protein surfaces had little or no effect on activity. One should also note that Ala residues are not only the most abundant but also the most conserved residues in the various AFP type I isoforms identified in winter flounder and sculpin. Also, this face is the most hydrophobic surface in the protein, which correlates well with the dominant energetic role of van der Waals interactions in the protein−ice adsorption. Even though this binding face has not been found here to be the preferred adsorption face on the [20$\bar{2}$1] planes, it may be an efficient surface adsorption face of the HPLC6. This protein surface has been involved in all other models generated, and it is further sterically very similar to the Thr-Ala-Asn face. This includes the macroscopic planarity as noted by Yang et al.,[20] as well as the surface corrugation and surface area (highlighted in Figure 4).

In conclusion, we could show that Monte Carlo calculations are able to generate unbiased and favorable adsorption models of HPLC6 to a number of selected ice-surface planes. These models will be invaluable starting structures for more detailed modeling studies such as dynamics calculations with explicit water treatment. Such studies are under way in several laboratories. Further, the analysis of the presented models suggest that van der Waals interactions are the major source of favorable intermolecular energy and lead to large orientational preferences in HPLC6−ice interactions. Nevertheless, van der Waals interactions are not sufficient to reproduce experimentally observed binding specificity, which suggest that electrostatic and hydrogen bond interactions may contribute to the protein−ice specificity.

Coordinates for all models are available at http://biophysics.cwru.edu/~frank/type1model.

ACKNOWLEDGMENT

We would like to thank Richard Laursen, Boston, for making the program for creating ice lattices available to us.

This work was supported by NIH Grant GM55362.

REFERENCES AND NOTES

(1) Raymond, J. A.; DeVries, A. L. Adsorption inhibition as a mechanism of freezing resistance in polar fishes. *Proc. Natl. Acad. Sci. U.S.A.* **1977**, *74* (6), 2589−2593.
(2) Davies, P. L.; Sykes, B. D. Antifreeze proteins. *Curr. Opin. Struct. Biol.* **1997**, *7* (6), 828−834.
(3) Yang, D. S. C.; Sax, M.; Chakrabartty, A.; Hew, C. L. Crystal structure of an antifreeze polypeptide and its mechanistic implications. *Nature* **1988**, *333*, 232−237.
(4) Wen, D.; Laursen, R. A. Structure−function relationships in an antifreeze polypeptide. The role of neutral, polar amino acids. *J. Biol. Chem.* **1992**, *267* (20), 14102−14108.
(5) Sicheri, F.; Yang, D. S. C. Ice-binding structure and mechanism of an antifreeze protein from winter flounder. *Nature* **1995**, *375*, 427−431.
(6) Knight, C. A.; Cheng, C. C.; DeVries, A. L. Adsorption of alpha-helical antifreeze peptides on specific ice crystal surface planes. *Biophys. J.* **1991**, *59* (2), 409−418.
(7) DeVries, A. L.; Lin, Y. Structure of a peptide antifreeze and mechanism of adsorption to ice. *Biochim. Biophys. Acta* **1977**, *495* (2), 388−392.
(8) Sönnichsen, F. D.; DeLuca, C. I.; Davies, P. L.; Sykes, B. D. Refined solution structure of type III antifreeze protein: Hydrophobic groups may be involved in the energetics of the protein-ice interaction. *Structure* **1996**, *4* (11), 1325−1337.
(9) Chao, H.; Houston, M. E., Jr.; Hodges, R. S.; Kay, C. M.; Sykes, B. D.; Loewen, M. C.; Davies, P. L.; Sönnichsen, F. D. A diminished role for hydrogen bonds in antifreeze protein binding to ice. *Biochemistry* **1997**, *36*, 14652−14660.
(10) Haymet, A. D.; Ward, L. G.; Harding, M. M. Winter flounder "antifreeze" proteins: Synthesis and ice growth inhibition of analogues that probe the relative importance of hydrophobic and hydrogen-bonding interactions. *J. Am. Chem. Soc.* **1999**, *121*, 941−948.
(11) Zhang, W.; Laursen, R. A. Structure−function relationships in a type I antifreeze polypeptide. The role of threonine methyl and hydroxyl groups in antifreeze activity. *J. Biol. Chem.* **1998**, *273* (52), 34806−34812.
(12) Baardsnes, J.; Kondejewski, L. H.; Hodges, R. S.; Chao, H.; Kay, C.; Davies, P. L. New ice-binding face for type I antifreeze protein. *FEBS Lett.* **1999**, *463* (1−2), 87−91.
(13) Wen, D.; Laursen, R. A. A model for binding of an antifreeze polypeptide to ice. *Biophys. J.* **1992**, *63* (6), 1659−1662.
(14) Lal, M.; Clark, A. H.; Lips, A.; Ruddock, J. N.; White, D. N. J. Inhibition of ice crystal growth by preferential peptide adsorption: a molecular modelling study. *Faraday Discuss.* **1993**, *95*, 299−306.
(15) Madura, J. D.; Wierzbicki, A.; Harrington, J. P.; Maughon, R. H.; Raymond, J. A.; Sikes, C. S. Interactions of the D- and L-forms of winter flounder antifreeze peptide with the {201} planes of ice. *J. Am. Chem. Soc.* **1994**, *116*, 417−418.
(16) Cheng, A.; Merz, K. M., Jr. Ice-binding mechanism of winter flounder antifreeze proteins. *Biophys. J.* **1997**, *73* (6), 2851−2873.
(17) Ding, H. Q.; Karasawa, N.; Goddard, W. A., III. Atomic level simulations on a million particles: The cell multipole method for Coulomb and London nonbond interactions. *J. Chem. Phys.* **1992**, *97*, 4309.
(18) Nicholls, A.; Sharp, K. A.; Honig, B. Protein folding and association: Insights from the interfacial and thermodynamic properties of hydrocarbons. *Proteins* **1991**, *11* (4), 281−296.
(19) Wierzbicki, A.; Taylor, M. S.; Knight, C. A.; Madura, J. D.; Harrington, J. P.; Sikes, C. S. Analysis of shorthorn sculpin antifreeze protein stereospecific binding to (2−1 0) faces of ice. *Biophys. J.* **1996**, *71* (1), 8−18.
(20) Yang, D. S. C.; Hon, W. C.; Bubanko, S.; Xue, Y.; Seetharaman, J.; Hew, C. L.; Sicheri, F. Identification of the ice-binding surface on a type III antifreeze protein with a "flatness function" algorithm. *Biophys. J.* **1998**, *74* (5), 2142−2151.

CI000449B